Comparison of Crystal and Solution Hemoglobin Binding of Selected Antigelling Agents and Allosteric Modifiers†

Ahmed S. Mehanna and Donald J. Abraham*

Department of Medicinal Chemistry, School of Pharmacy, Medical College of Virginia, Virginia Commonwealth University, P.O. Box 581, MCV Station, Richmond, Virginia 23298

Received March 29, 1989; Revised Manuscript Received December 20, 1989

ABSTRACT: This paper details comprehensive binding studies (solution and X-ray) of human hemoglobin A with a group of halogenated carboxylic acids that were investigated as potential antisickling agents. It is, to our knowledge, the first study to compare solution and crystal binding for a series of compounds under similar high-salt conditions used for cocrystallization. The compounds include [(3,4-dichlorobenzyl)oxy]acetic acid, [(*p*-bromobenzyl)oxy]acetic acid, clofibric acid, and bezafibrate. The location and stereochemistry of binding sites have been established by X-ray crystallography, while the number of binding sites and affinity constants were measured by using equilibrium dialysis. The solution binding studies were conducted with deoxygenated hemoglobin and carbonmonoxyhemoglobin with low (50 mM) and high (2 M) salt concentrations. It was concluded that the observed crystal structures are consistent with the binding observed in solution and that the number of binding sites is independent of salt concentration, while the binding constant increases with increasing salt concentration. The studies also reveal that relatively small changes in the chemical structure of a drug molecule can result in entirely different binding sites on the protein. Moreover, the X-ray studies provide a possible explanation for the multiplicity in function exhibited by these compounds as allosteric modulators and/or antisickling agents. Finally, the studies indicate that these compounds bind differently to the R and T states of hemoglobin, an observation of special significance to the original design of these agents.

Among the newly discovered potential antisickling agents are the (benzyloxy)acetic acid derivatives [(3,4-dichlorobenzyl)oxy]acetic acid (DCBAA,[1] compound **1**) and [(*p*-bromobenzyl)oxy]acetic acid (BBAA, compound **2**) (Abraham

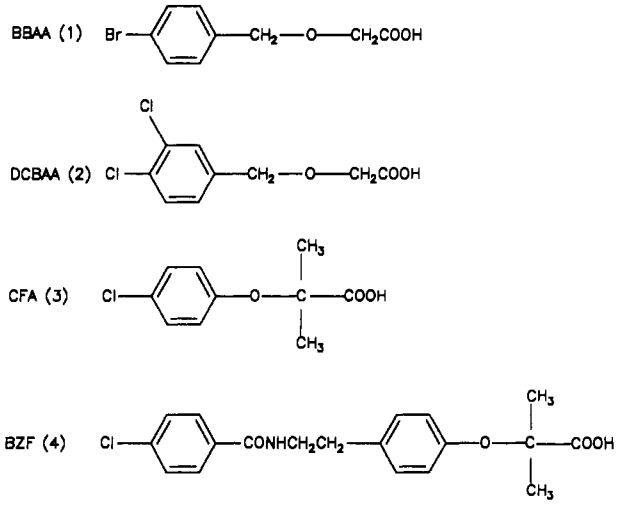

et al., 1982, 1984). The compounds showed remarkable antigelling activity when tested by the C-sat assay developed by Hofrichter and co-workers (Hofrichter et al., 1976). These results suggested that we test the well-known antilipidemic drug clofibric acid (CFA, compound **3**). Likewise, Perutz suggested bezafibrate (BZF, compound **4**), another antilipidemic agent, for evaluation as an antisickling agent and allosteric modulator. Clofibric acid showed moderate antigelling activity, while bezafibrate was found to be progelling at low concentrations (Abraham et al., 1984). BZF, however, did show antigelling properties at higher concentrations (above 20 mM) (Abraham et al., 1984).

The overall observed order of activity for the four compounds as antigelling agents was **1** > **2** > **3** > **4**. Conversely, the ability of the same compounds to decrease the oxygen affinity of Hb (shift the allosteric equilibrium to the right) was reversed: **4** > **3**, while **2** and **1** had little to no effect. This reciprocal order of antigelling activity vs allosteric modulation suggested that we further investigate the binding characteristics of these compounds. Therefore, studies were conducted to determine or compare the following characteristics:

(1) Do the compounds bind differently to deoxyhemoglobin (dxHb) and carbonmonoxyhemoglobin (HbCO)?

(2) What are the number of classes of binding sites, the number of drug molecules bound to each class of sites, and the binding constant for each class using Scatchard plot methodology?

(3) What are the locale and stereochemistry of binding? This was elucidated by X-ray analyses of crystals obtained by cocrystallization of hemoglobin with the four compounds. This paper focuses on the locale and number of binding sites. The stereochemistry of binding has appeared elsewhere (Abraham et al., 1983, 1984; Perutz et al., 1986).

(4) Is the observed cocrystallization-state binding at high salt concentration consistent with the observed solution-state binding under low-salt (physiological) conditions? Accordingly, solution binding studies were conducted at both low and

†Grant support of this work from NIH-HLBI-RO1-32793 is acknowledged.

[1] Abbreviations: BBAA, [(*p*-bromobenzyl)oxy]acetic acid; DCBAA, [(3,4-dichlorobenzyl)oxy]acetic acid; CFA, clofibric acid; BZF, bezafibrate; HbCO, carbonmonoxyhemoglobin; dxHb, deoxyhemoglobin; R, relaxed state of hemoglobin; T, tense state of hemoglobin.

0006-2960/90/0429-3944$02.50/0

Table I: Experimental Conditions of the Equilibrium Dialysis Procedure

compound	buffer concn	Hb state	Hb concn[a] (mM)	drug[b] concn range (mM)	method of analysis
DCBAA	50 mM	HbCO	1.74	0.25–34.0	UV
DCBAA	50 mM	dxHb	3.15	0.25–8.0	HPLC
DCBAA	2.0 M	HbCO	0.86	0.25–7.0	UV
DCBAA	2.0 M	dxHb	0.30	0.025–0.5	HPLC
BBAA	50 mM	HbCO	2.75	0.25–5.0	HPLC
BBAA	50 mM	dxHb	3.15	0.25–4.0	HPLC
CFA	50 mM	HbCO	2.73	0.25–6.0	HPLC
CFA	50 mM	dxHb	3.15	0.25–8.0	HPLC
BZF	50 mM	HbCO	1.61	0.25–10.0	UV
BZF	50 mM	dxHb	3.60	0.25–6.0	HPLC
BZF	1.6 M	dxHb	0.10	0.025–0.5	HPLC

[a] Hemoglobin concentration injected into the dialysis cells. In the calculation of the molar binding ratios, these concentrations were corrected to the total cell volume (0.6 mL) via division by 2 and 3 in HbCO and dxHb studies, respectively. [b] Range of drug concentrations after equilibrium and as determined from control cells.

high salt concentrations in cases where the low-salt data indicated specific binding.

(5) What is the relationship between the locale of binding and the observed activity of these compounds as antigelling agents and allosteric modulators?

Materials and Methods

BBAA and DCBAA were prepared as previously reported (Abraham et al., 1982). CFA was purchased from Aldrich, while BZF was kindly provided by Dr. Max Perutz, MRC Laboratories, Cambridge, U.K.

Human blood was obtained as NSQ units from the Central Blood Bank of Pittsburgh, Pittsburgh, PA.

The phosphate buffer employed for the low-salt studies was 50 mM, pH 7.4, isotonic, and iso-osmotic to which 100 mM sodium chloride was added to eliminate the Donnan equilibrium effect. For high-salt studies, the phosphate buffer (pH 7.4) concentration was 2 M for DCBAA and 1.6 M for BZF (due to solubility problems with BZF in 2 M buffer).

Equilibrium dialysis studies were performed by using an equilibrium microvolume dialyzer (Hoffer Scientific Instruments, Model EMD101 0.5 mL) fitted with 3-in.-diameter and 12000–14000-Da cutoff dialysis membranes (Hoffer Scientific Instruments EMD103). The dialysis membranes were prepared as described below.

Two analytical techniques were employed to measure the concentration of free drug after equilibrium dialysis. In the carbonmonoxy studies (except for BBAA and CFA), free drug concentrations were measured by direct UV analysis using a Beckman UV spectrophotometer (Model 25). It should be noted that after HbCO binding, the analysis of free drug concentration using UV and HPLC gave identical results within experimental error. The method of analysis described in Table I is based on experiments with the largest number of runs and data points. In the deoxy studies, high-performance liquid chromatography (HPLC) was used to analyze and separate the drug from excess dithionite, which has a high background signal in the UV range used.

The HPLC system (Waters) was equipped with a U6K injector, a variable-wavelength detector (Waters, Model 450), solvent programmer (Waters, Model 660), and computerized integrator (HP, Model 3392A). The wavelengths monitored during HPLC analyses were first determined with a Varian spectrophotometer (Model DMS-100) fitted with a Varian (Model DS-15) data station. A Waters reverse-phase, prepacked, 30 cm × 4 mm i.d., stainless steel column containing

Table II: Wavelength of Maximum Absorption and the Corresponding Extinction Coefficient of Compounds Analyzed by Direct UV

compound	buffer concn	Hb state	wavelength (nm)	molar extinction coefficient/10^3
DCBAA	50 mM	HbCO	216	9
BZF	50 mM	HbCO	225	18
DCBAA	2.0 M	HbCO	216	9

μBondapak C-18 material generating 12000 plates/m was employed. A guard column (60 mm × 3.9 mm) packed with the same material but possessing a larger particle size was used to increase the column lifetime.

Procedures. Pure hemoglobin A was prepared under conditions previously described (Abraham et al., 1984) and equilibrated with the appropriate buffer (50 mM for low-salt studies and 1.6 or 2 M phosphate for high-salt studies). For the HbCO binding studies, CO was bubbled through the hemoglobin solution for 30 min. If the UV absorbencies at 540 and 569 nm were not equal, the solution was reduced with dithionite followed by further treatment with CO until both absorptions were equal (Perutz, 1968).

Dialysis membranes were boiled with a 5% sodium carbonate–50 mM EDTA solution for 5 min and then washed twice with distilled water and stored in 50% ethanol at 4 °C. Membranes were rehydrated before use by soaking in dialysis buffer overnight. The time required to attain equal concentration on both sides of the membrane (equilibrium time) was determined for each compound. In all cases it was found to be below 3 h.

For binding studies to HbCO, one chamber of the dialysis cell was filled with 0.3 mL of HbCO (known concentration) and the other chamber with 0.3 mL of a given drug concentration. Control sets of cells were filled by injecting the same volume (0.3 mL) of a given drug concentration in one chamber and 0.3 mL of buffer in the other chamber. After the chambers were filled, the whole system was rotated at 4 °C for 20–24 h.

The same procedure and apparatus were used for dxHb binding studies with the following modification: a dithionite concentration of 100 mM [see Dalziel and O'Brien (1957a,b)] was maintained by charging each chamber with 0.1 mL of sodium dithionite solution (prepared at a concentration of 300 mM in degassed, pH 7.4, phosphate buffer) and 0.2 mL of drug solution, 0.2 mL of HbA, or 0.2 mL of buffer for the control cells. The cells were immediately sealed with Vaseline and parafilm before rotation for 20–24 h at 4 °C. Table I summarizes the experimental conditions of the equilibrium dialysis procedure. After the equilibrium period, the concentration of the drug in both test and control cells was measured by either UV absorbance or HPLC. The concentration of the drug in the control dialysis cells was routinely compared with the concentration of the corresponding solution used for filling the same cells. No indication of drug binding to non-protein materials was observed. Tables II and III summarize compounds and conditions for direct UV and HPLC analyses, respectively.

Scatchard Plots. The Scatchard plot (Scatchard, 1949) is one of the most popular methods to analyze ligand–protein interactions. The method is based on the equation

$$r/C_f = nK - Kr \quad (1)$$

where r is the molar binding ratio, i.e., moles of drug bound per mole of protein; C_f is the molar concentration of free (unbound) drug; n is binding-site multiplicity per class of binding site; and K is the equilibrium binding constant.

Table III: Experimental Conditions of HPLC Analyses

compound	buffer concn	Hb state	mobile phase[a] (% CH_3CN)	RT[b] (min)	IS[c] compound	IS[c] RT	WL[d] (nm)
DCBAA	50 mM	dxHb	30	4.6	BBIA	6.6	215
DCBBA	2.0 M	dxHb	25	6.5	BZF	10.0	225
BBAA	50 mM	dxHb	25	4.4	CFA	6.8	219
BBAA	50 mM	HbCO	25	4.4	CFA	7.0	219
CFA	50 mM	HbCO	27	5.3	BBIA	7.9	225
CFA	50 mM	dxHb	27	5.4	BBIA	7.8	225
BZF	50 mM	dxHb	30	7.9	DCBAA	4.9	225
BZF	1.6 M	dxHb	27	9.0	DCBAA	5.4	225

[a] Mobile phase was always acetonitrile in distilled water acidified with acetic acid (1.4 mL/L of H_2O). [b] RT stands for retention time. [c] IS stands for internal standard, which was usually prepared in the same buffer except for high-salt studies, for which it was prepared in 50% glacial acetic acid. BBIA stands for 2-[(*p*-bromobenzyloxy)]isobutyric acid. [d] WL is the wavelength of maximum absorption determined in the corresponding mobile phase.

Table IV: Summary of the Results Obtained from Solution Binding Studies[a]

compound	salt concn	no. of molecules per class/Hb tetramer (n)[b]	$(K)/10^3$[d] (M^{-1})	$nK/10^3$[c] (M^{-1})
DCBAA to HbCO	low	6.0 (5.7)	0.11 (0.11)	0.64 (0.63)
		nonspecific binding		0.12 (0.11)
DCBAA to dxHb	low	1.5 (1.6)	0.67 (0.62)	1.00 (0.99)
		nonspecific binding		0.15 (0.15)
DCBAA to HbCO	high (2 M)	6.0 (6.0)	0.73 (0.63)	4.40 (3.78)
		nonspecific binding		0.75 (1.29)
DCBAA to dxHb	high (2 M)	1.6 (1.7)	2.85 (2.58)	4.56 (4.39)
		nonspecific binding		0.58 (0.60)
BBAA to HbCO	low	nonspecific binding		0.45
BBAA to dxHb	low	nonspecific binding		0.34
CFA to HbCO	low	nonspecific binding		0.28
CFA to dxHb	low	1.5 (1.5)	0.29 (0.29)	0.44 (0.44)
		2.0 (2.0)	0.06 (0.06)	0.11 (0.11)
		nonspecific binding		0.03 (0.03)
BZF to HbCO	low	nonspecific binding		0.30
BZF to dxHb	low	2.3 (2.2)	0.61 (0.57)	1.40 (1.25)
		4.8 (5.9)	0.13 (0.12)	0.62 (0.71)
BZF to dxHb	high (1.6 M)	1.6 (1.5)	18.75 (17.0)	30.0 (25.5)
		5.5 (5.2)	1.36 (1.66)	7.48 (8.60)

[a] These values are derived from graphical analysis; those obtained by the LIGAND program are in parentheses. [b] Intercept on the x axis. [c] Intercept on the y axis. [d] Calculated from nk/n.

For the ideal case of a single class of binding sites, a plot of r/C_f versus r displays a straight line where the x-axis intercept is n and the y-axis intercept is nK. The equilibrium constant K (slope) is easily calculated from these two parameters.

Curvature of a Scatchard plot implies either that there is more than one class of binding sites (with each class characterized by a unique number of binding sites and association constant) or the binding of each successive molecule alters the association constant of the next molecule (Scheinberg, 1982; Scheinberg & Armstrong, 1950). In nonlinear Scatchard plots, where different classes of binding sites are simultaneously competing for the same pool of ligand, the binding equilibrium is governed (at any data point) by

$$r/C_f = (n_1K_1 - r_1K_1) + (n_2K_2 - r_2K_2) + \ldots (n_xK_x - r_xK_x) \quad (2)$$

where r is the total molar binding ratio (experimentally observed), C_f is the molar concentration of free (unbound) ligand, and r_x is the molar binding ratio incorporated by the (x) binding class of K_x binding constant and n_x multiplicity of binding sites.

The determination of the binding parameters for each individual class of binding sites requires a mathematical resolution of eq 2. Accordingly, several methods (Rosenthal, 1967; Pennock, 1973; Blondeau & Robel, 1975; Munson & Rodbard, 1980; Kent et al., 1980; Molinoff et al., 1981) have been developed to deconvolute curved Scatchard plots and calculate the binding parameters of individual classes.

Calculations. In the present binding studies most of the plots exhibited a nonlinear profile, which indicates either multiple classes of binding sites or negative cooperativity. The X-ray findings (vide infra) support the first assumption, although negative cooperativity cannot be fully excluded.

Scatchard plots were resolved into individual binding curves by using the graphical approach developed by Rosenthal (1967) and automated by Pennock (1973). The LIGAND program developed by Munson and Rodbard (1980) was also used whenever the plots demonstrated specific binding. Both analytical approaches produced the same binding parameters. Binding parameters calculated by both methods are summarized in Table IV. The numerical values used throughout the following discussion are those derived by using Rosenthal's graphical approach.

The graphical method to resolve nonlinear Scatchard plots is a trial and error procedure to determine the individual "binding lines". For each class of binding, the binding-site multiplicity (n) and nK are the x and y intercepts, respectively. The binding constant (K) could be calculated from y/x. The end point of the refinement procedure is the point at which the theoretically calculated curve (according to eq 2 or by addition of the radial lines from the origin to each binding line) matches the experimental curve [for more details, see Rosenthal (1967) and Pennock (1973)].

It should be noted that whenever the plots demonstrated nonspecific class of sites, only nK could be calculated for that particular class. Accordingly, for DCBAA binding (Figure 1) where two classes of binding sites are observed, one of which

is nonspecific, a simplified form of eq 2 was applied:

$$r/C_f = (n_1K_1 - r_1K_1) + n_2K_2 \quad (3)$$

Likewise, in the case of CFA (Figure 3), which appears to have three classes of binding sites, one of which is nonspecific, eq 4 was applied:

$$r/C_f = (n_1K_1 - r_1K_1) + (n_2K_2 - r_2K_2) + n_3K_3 \quad (4)$$

It should be further noted that n_2K_2 and n_3K_3 in eqs 3 and 4, respectively, represent the participating fractions of the corresponding total nonspecific sites in the binding process before saturation of specific binding sites (Blondeau & Robel, 1975). The implication of this fact on the curve-fitting procedure is that eqs 3 and 4 apply only up to the point where the curve levels off. The latter represents the saturation point of the specific class(es) of binding sites, after which r/C_f is sustained by further binding to the nonspecific sites.

Hemoglobin Structure. Hb is a tetramer with two α and two β subunits. A molecular twofold axis bisects the tetramer. Therefore, a drug binding site on one subunit will have an identical binding site on the other subunit. For example, a molecule bound at Trp-14α 1 will have another equal potential binding site at Trp-14α 2. The Trp-14α binding site would be considered a single class of binding site that can bind a total of two molecules. In some instances, a molecule can bind to both subunits simultaneously, such that the small molecule bisects the twofold axis. Diphosphoglyceric acid (DPG), the natural allosteric effector of Hb, is such a molecule. One molecule of DPG bisects the β subunits (and the twofold axis), making two ionic interactions with one β subunit and one with the other (Arnone, 1972). Therefore, the DPG binding site would be considered one class with one molecule maximum occupancy. In deoxygenated hemoglobin (T state), the subunits are arranged so that a central water cavity cleft exists that exposes potential binding sites for small molecules. In oxygenated (R state) hemoglobin, the subunits are rearranged so that the central water cavity around the molecular twofold axis is narrowed and the potential binding sites are not exposed.

Results

Solution Binding Studies. Solution binding studies were carried out under normal physiological conditions and in certain cases under the high salt concentrations used for cocrystallization. Figures 1, 2, 3, and 4 are Scatchard plots of DCBAA, BBAA, CFA, and BZF, respectively under the different experimental conditions of low and high salt concentrations and HbCO vs dxHb.

DCBAA (the most extensively studied compound) showed distinct binding properties (Figure 1). It was found to bind differently to R (HbCO) and T (dxHb) states of hemoglobin. The Scatchard plot of DCBAA binding to HbCO under low salt concentration (Figure 1A) shows two classes of binding sites (primary and secondary). The primary binding sites (6.0 multiplicity) were specific saturable sites with a very weak binding constant (0.11×10^3 M^{-1}). The secondary binding sites were nonspecific and nonsaturable with an nK value of 0.12×10^3 M^{-1}. DCBAA binding to dxHb in low salt (Figure 1A) was found to be completely different with regard to both the number and affinity of binding sites. DCBAA has approximately two primary saturable binding sites (one class) with a considerably higher binding constant (0.67×10^3 M^{-1}) and nonsaturable sites with an nK value of 0.15×10^3 M^{-1}.

On the other hand, results of DCBAA binding studies at high salt concentrations to both HbCO and dxHb (Figure 1B) indicate that the numbers of binding sites were the same as

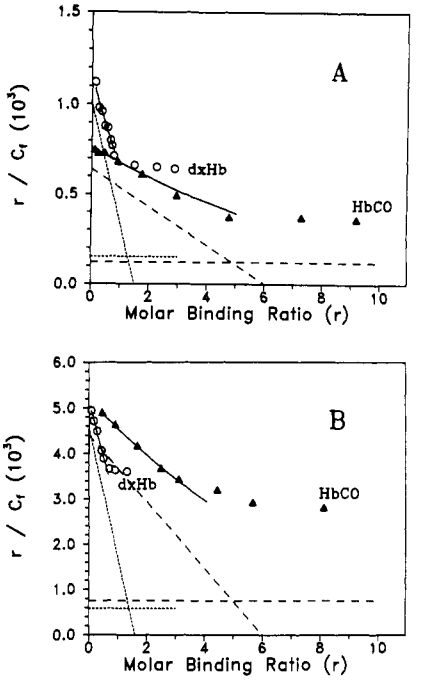

FIGURE 1: Scatchard plots of DCBAA binding with HbCO and dxHb: (A) under low-salt conditions; (B) under high-salt conditions. The experimental data are displayed as discrete points. The dashed and dotted lines represent the resolved binding lines for HbCO and dxHb, respectively. The solid lines represent the theoretical curves calculated by the addition of radial lines between the origin and the resolved binding lines. For the significance of the horizontal data points, see text.

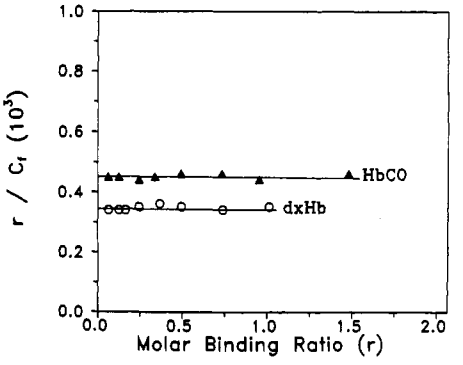

FIGURE 2: Scatchard plots of BBAA binding with HbCO and dxHb under low-salt conditions. The experimental data are displayed as discrete points. The solid lines represent average nK values.

those observed with the low-salt studies (6 and 1.6, respectively). However, the binding constants were notably higher (a 7-fold increase with HbCO and a 4-fold increase with dxHb). See Table IV for comparison.

BBAA did not exhibit specific binding characteristics (Figure 2). Only nonspecific binding was observed with both HbCO and dxHb exhibiting weak nK values (0.45×10^3 and 0.34×10^3 M^{-1}, respectively).

CFA binding to HbCO at low salt concentration (Figure 3) was also found to be nonspecific with a weak nK value (0.28×10^3 M^{-1}). However, its binding to dxHb at low salt concentration was rather complicated and nonlinear, indicating multiple classes of binding sites. The Scatchard plot (Figure 3) suggests three classes of binding sites: a primary class (1.5 molecules) with K of 0.29×10^3 M^{-1}; a secondary class (2.0 molecules) with K of 0.06×10^3 M^{-1}); and nonspecific sites with nK of 0.03×10^3 M^{-1}. However, the proposed deconvolution of these data is somewhat conditional due to the small number of experimental measurements possible in the narrow

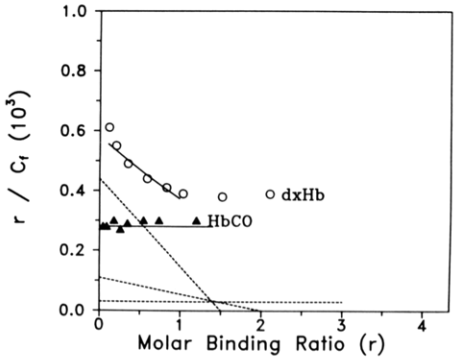

FIGURE 3: Scatchard plots of CFA binding with HbCO and dxHb under low-salt conditions. The experimental data are displayed as discrete points. For dxHb, the dotted lines represent the resolved binding lines and the solid line represents the theoretical curve calculated by the addition of radial lines between the origin and the resolved binding lines. In the HbCO case, the solid line represents an average nK.

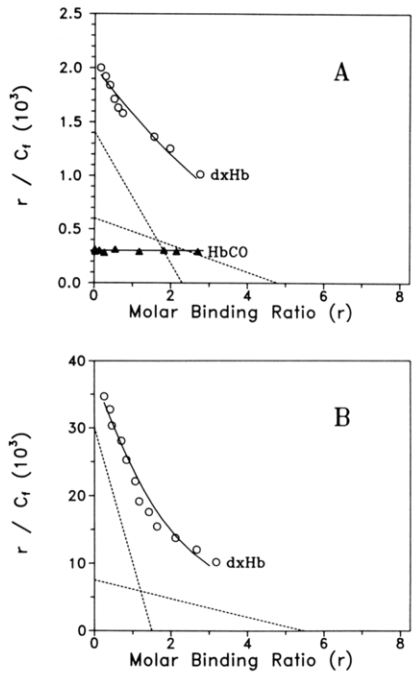

FIGURE 4: Scatchard plots of BZF binding: (A) with HbCO and dxHb under low-salt conditions; (B) with dxHb under high-salt conditions. The experimental data are displayed as discrete points. For dxHb, the dotted lines represent the resolved binding lines and the solid lines represent the theoretical curves calculated by the addition of radial lines between the origin and the resolved binding lines. In the HbCO case, the solid line represents an average nK.

concentration range observed. The overall conclusion from solution CFA binding studies to dxHb is that CFA has multiple classes of binding sites with close binding affinities. The X-ray studies (vide infra) confirm the occurrence of multiple binding sites.

BZF was also extensively studied. At low salt concentration, HbCO–BZF showed only a weak nonspecific binding (nK = 0.30×10^3 M^{-1}), while under low-salt conditions with dxHb, BZF was found to have two classes of saturable binding sites (Figure 4A). Figure 4A demonstrates a primary class (2.3 sites) with a relatively high binding constant (0.61×10^3 M^{-1}) and a secondary class (4.8 sites) with a lower binding constant (0.13×10^3 M^{-1}).

BZF binding under high-salt conditions was conducted only with dxHb (Figure 4B) since it binds nonspecifically to HbCO under low-salt conditions. BZF high-salt binding studies revealed approximately similar numbers of binding sites as those

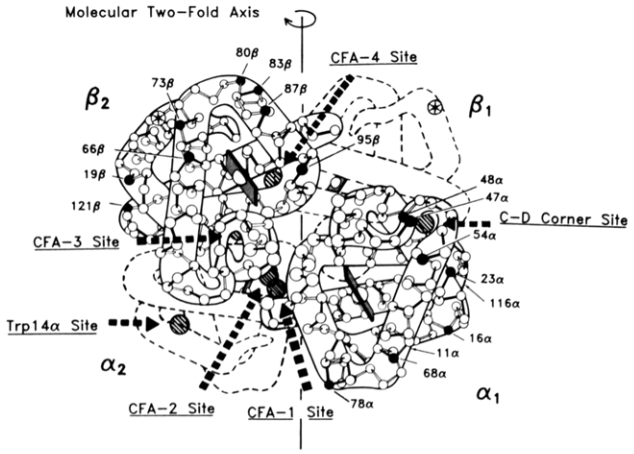

FIGURE 5: Schematic of hemoglobin molecule indicating the Trp-14α, C-D corner, and central water cavity binding sites. With the exception of the asymmetric C-D corner binding, each binding site has another site on the hemoglobin tetramer that is not indicated on the figure but is related by the molecular twofold. The star on the β chain represents the mutation site in hemoglobin S (6βGlu-Val). The amino acid residues with solid circles represent areas of the molecule involved in the HbS polymer contacts and are labeled as reference points to the binding sites.

observed in the low-salt studies (1.6 sites for primary and 5.5 for secondary); however, the binding constants under high-salt conditions were considerably higher (18.75×10^3 and 1.36×10^3 M^{-1}, respectively).

X-ray Findings. All compounds were cocrystallized with both dxHb and HbCO under conditions previously described (Perutz, 1968).

(*a*) *Carbonmonoxyhemoglobin Binding.* Unfortunately X-ray crystallographic analyses of HbCO with these agents have not proved informative. Good crystals were obtained for BZF and CFA when cocrystallized with HbCO, but the drugs were not located in the R-state crystal analyses [see Perutz et al. (1986) for BZF and Abraham et al. (1983) for CFA]. BBAA and DCBAA produced crystals of poor quality. The former were twinned, while the latter molecule induced a change in HbCO crystal morphology from tetragonal to orthorhombic. The orthorhombic DCBAA crystals diffracted poorly.

(*b*) *Deoxyhemoglobin Binding.* We have been able to make good use of deoxyhemoglobin crystals (grown in concentrated salt solution) to monitor the binding of these agents. As indicated earlier, the present paper focuses on the locale and number of binding sites, and the stereochemistry of binding is described elsewhere (Abraham et al., 1983, 1984; Perutz et al., 1986). The major classes of binding sites discussed here are shown in Figure 5.

Four of these sites are located in the water-filled central cavity, and all four sites were found to be occupied by molecules of clofibric acid (CFA). Therefore, these sites have been designated CFA1, CFA2, CFA3, and CFA4. CFA1 and CFA2 are major sites with high occupancy (Figure 6A), while CFA3 and CFA4 are minor sites with low occupancy (Figure 6B).

Two other major sites for binding halogenated aromatic compounds are located near the surface of the molecule and are designated the Trp-14α site and the C-D corner site. In deoxy crystals, DCBAA is exclusively bound at the Trp-14α site (Figure 7A,B). The C-D corner site is occupied by BBAA [one major asymmetric binding site of relatively high density (Figure 8)]. Two minor low-occupancy classes were also observed for BBAA in the central water cavity and correspond to the CFA3 and CFA4 sites. BZF (1 molecule) was found

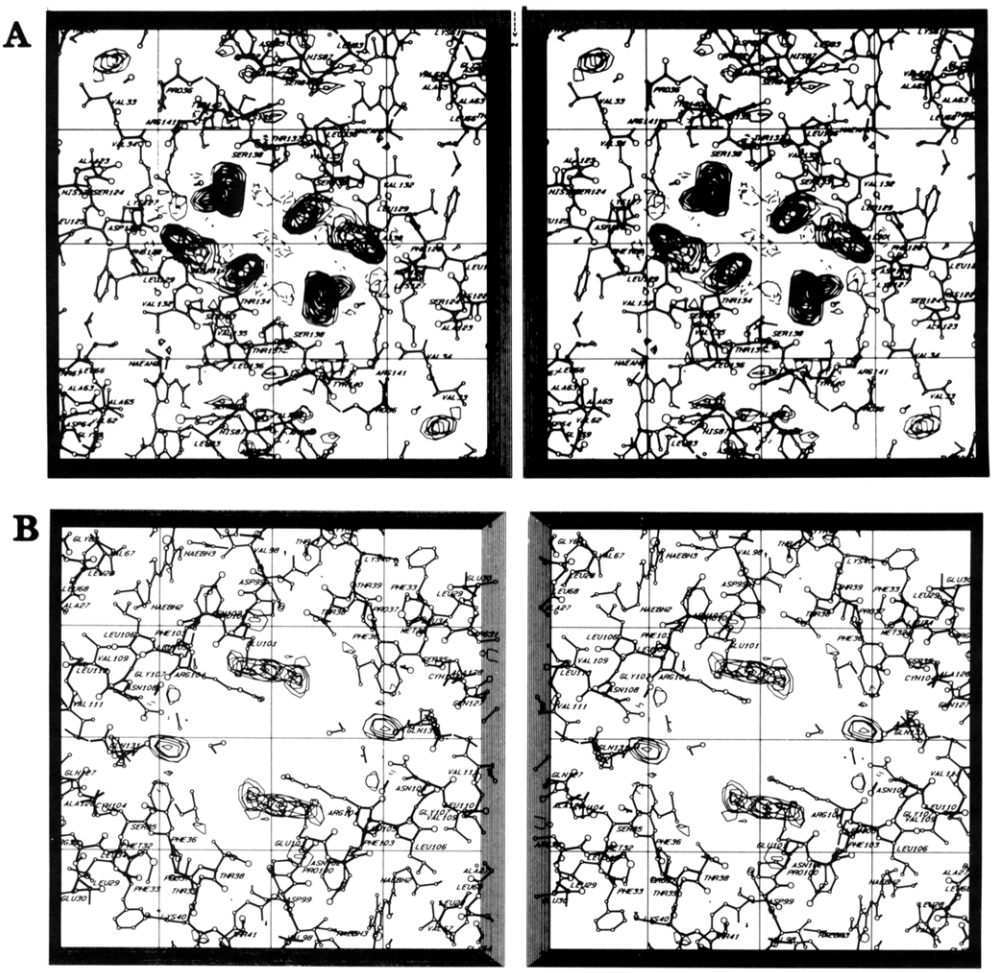

FIGURE 6: (A) Two primary binding sites (four molecules) for CFA in the central water cavity. The twofold axis bisects the two sites. Site CFA1 exhibits electron density for the two symmetrically related molecules (upper left and lower right). Site CFA2 is at the lower left and upper right portion of the central water cavity. (B) Two secondary binding sites further down the central water cavity near the α,β interface. Site CFA3 is located at the circular densities to the left and right of the twofold axis. The extended elliptically shaped densities at the top and bottom of the central water cavity depict site CFA4.

to occupy both the CFA1 and CFA3 sites with a net molar binding ratio of 2 molecules of BZF/hemoglobin tetramer (Figure 9A,B).

Discussion

R- and T-State Binding. The R-state solution binding studies indicate nonspecific binding (nonsaturable Scatchard plots) for BBAA, CFA, and BZF (Figures 2, 3, and 4A, respectively). The Scatchard plots of DCBAA–R state binding (Figure 1A,B) showed a large number of molecules (6.0) bound to one class of sites with a very low binding constant (weak binding). It is not surprising, then, considering the nonspecificity of CFA and BZF with solution HbCO studies, that X-ray crystal analyses did not produce distinct binding sites. As stated earlier, BBAA and DCBAA crystals were not suitable for X-ray analyses.

On the other hand, both X-ray and solution binding studies indicate that the compounds have more specific and informative binding to dxHb.

The preferential binding of these compounds to dxHb may have special significance since they were originally designed and tested to inhibit hemoglobin polymerization under deoxy conditions (Abraham et al., 1984).

Solution- and Crystal-State Binding. To our knowledge, this is the first comprehensive study that has evaluated solution binding and crystal binding of potential drug agents under the same high-salt cocrystallization conditions. The comparison of dxHb solution and crystal binding data is presented below. The number of binding sites (both solution and X-ray) and the locales of binding are summarized in Table V. These studies clearly demonstrate that the solution-state binding and the crystal-state binding of the four organic acids with dxHb are in agreement and are consistent with the interpretation that the X-ray maps reflect solution binding.

(*a*) [(*Dichlorobenzyl*)*oxy*]*acetic Acid.* Solution binding studies indicate one class of high-affinity binding sites with approximately 2 molecules bound/hemoglobin tetramer (Figure 1A). The difference electron density map (Figure 7A) clearly indicates one primary binding site at Trp-14α, which also accounts for 2 molecules of DCBAA/hemoglobin tetramer.

We conclude that solution binding studies and X-ray analysis of DCBAA are fully consistent.

(*b*) *Clofibric Acid.* The Scatchard plot of CFA binding to dxHb (Figure 3) indicates two poorly resolved classes of binding sites with a total number of 4 CFA molecules/hemoglobin tetramer (approximately 2 molecules bound to each class). The binding curve levels off near a 0.4×10^3 molar binding ratio/free drug concentration. This indicates other nonsaturable, nonspecific binding sites.

The X-ray difference map (Figure 6A) shows 4 molecules bound at two high-occupancy sites (CFA1 and CFA2). The two molecules in CFA1 are related by the twofold axis, as are the two bound at CFA2. The map also reveals two more minor

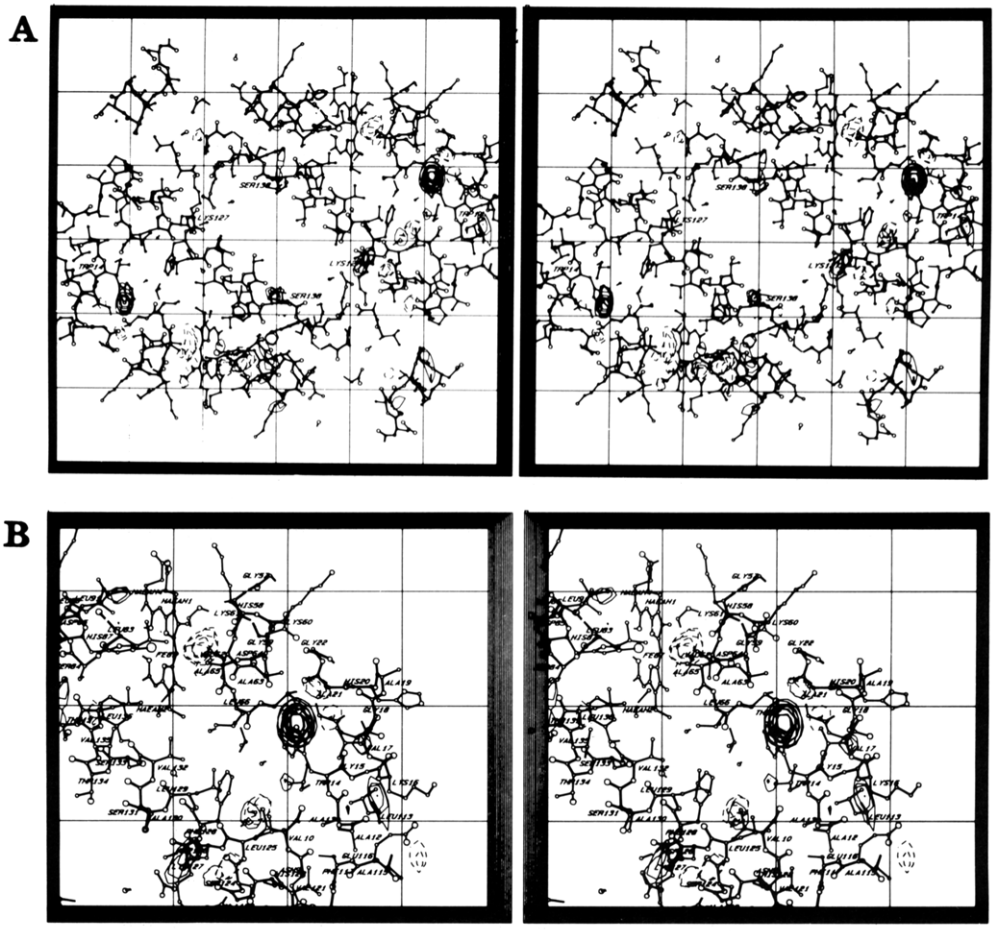

FIGURE 7: (A) Binding sites for DCBAA located at the Trp-14α residues near the outer edges of the map (upper right and lower left). This is a non symmetry average map so the densities of the two molecules are different in intensity. (B) Blowup of the Trp-14α site showing the need for the Trp to move to give rise to the binding pocket. No electron density was observed to indicate a new position for the Trp.

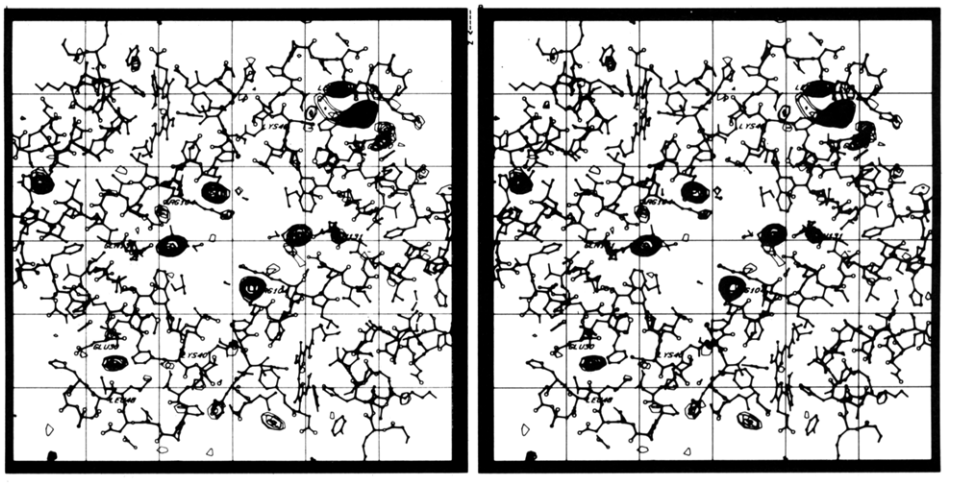

FIGURE 8: Asymmetric binding of BBAA with only one molecule at the C-D corner (upper right) of the map. The central water cavity shows secondary binding sites at CFA3 and CFA4 in the central water cavity.

classes of binding sites (CFA3 and CFA4) with two potential molecules at each site but with low occupancy (Figure 6B). Although CFA3 and CFA4 may be specific sites (from X-ray), they may appear in solution binding studies as nonspecific sites, probably due to their low K.

These results suggest that the solution binding (four molecules probably bound at two sites) agrees with the two high-occupancy sites (CFA1 and CFA2). The low-occupancy sites in the X-ray maps (at CFA3 and CFA4) are most probably accounted for in the nonspecific (weaker binding) portion of the Scatchard plot (Figure 3).

Both solution- and crystal-state binding studies agree that CFA binds to dxHb at multiple classes of binding sites.

(*c*) *[(p-Bromobenzyl)oxy]acetic Acid.* Figure 8 depicts the crystal binding of BBAA. The upper right corner of the electron density indicates one molecular of BBAA bound with a relatively high density at the C-D corner site, but the corresponding site related by the twofold axis has only very low density. We were surprised to see this asymmetric binding in the crystal structure and have speculated elsewhere (Abraham et al., 1984) that the BBAA site with relatively high density may result from crystal packing differences between

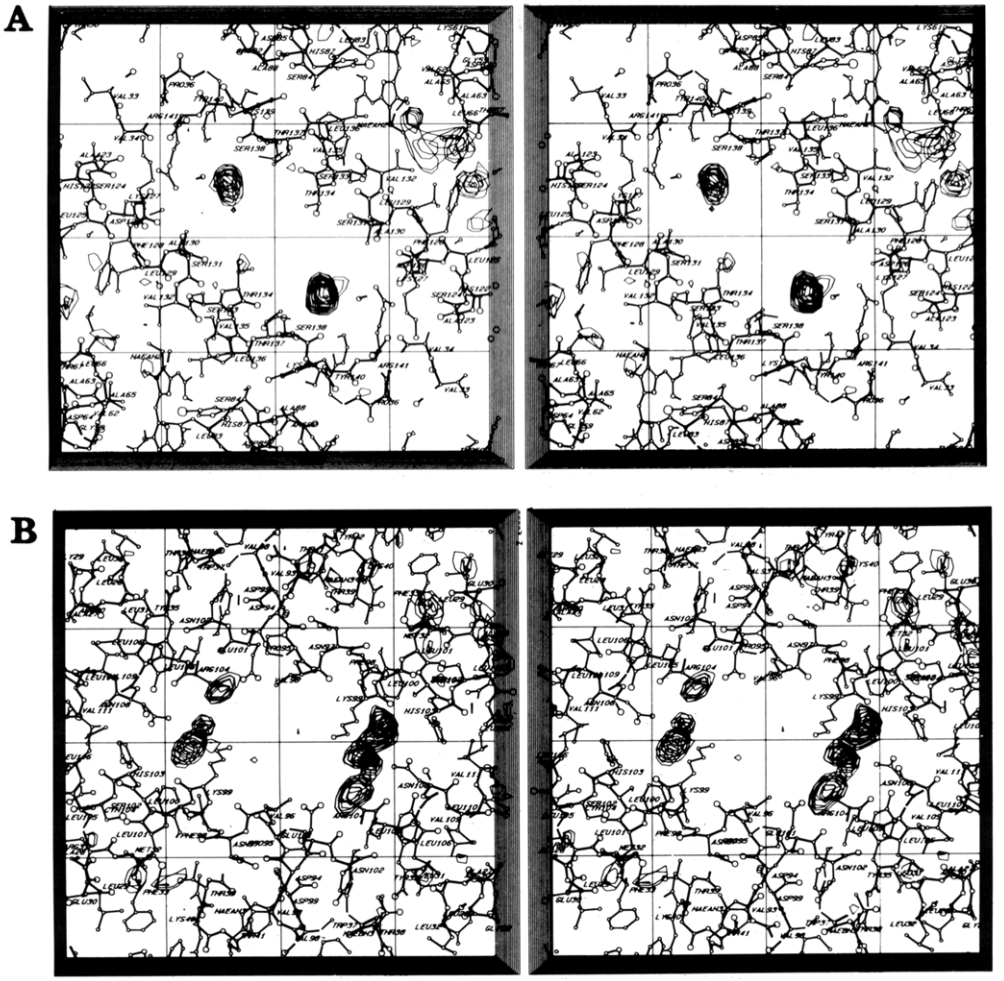

FIGURE 9: (A) Top half of BZF binding site (upper left and lower right) that overlaps the CFA1 site (see Figure 6A). (B) Bottom half of the BZF binding site that overlaps with the CFA3 site (see Figure 6B).

Table V: Comparison of Solution Binding Studies and X-ray Binding Data with dxHb

	solution binding studies			X-ray analysis		
compound	nature of binding[a]	no. of binding sites[b]	total no. of sites/Hb tetramer	occupancy	locale of binding	total no. of molecules/Hb tetramer
BBAA	nonsp	α	α	asymmetric	C-D corner	1
DCBAA	sp	2	2	primary	Trp-14α	2
	nonsp	α	α	secondary[c]		
CFA	sp	2	2	high	CFA1	2
	sp	2	2	high	CFA2	2
	nonsp	α	α	low	CFA3	2
				low	CFA4	2
BZF	sp	2	2	high	at both CFA1 and CFA3	2
	sp	5	5	low	Trp-14α	2
					Trp-15β	2

[a] Nonsp and sp denote nonspecific and specific binding, respectively. [b] From Table IV after rounding. [c] We did not fit the molecules for DCBAA and cannot comment on occupancy at these sites. The X-ray data for this derivative were not of high quality.

the two sites. We have interpreted the observed asymmetric binding as nonspecific binding since by definition specific binding should be manifested at both sites around the symmetry axis.

Figure 8 also depicts the central water cavity with two minor classes (low occupancy) of binding sites with two molecules at each site realted by the twofold axis. These BBAA minor sites were found to be superimposed (via graphics) with the minor sites found for CFA (CFA3 and CFA4).

Solution binding results revealed only nonspecific binding for BBAA (Figure 2). The absence of a distinct class of binding in solution studies may be attributed to weak binding. The difference electron density map at the C-D corner (asymmetric binding) and in the central water cavity sites (low occupancy) also suggests weak and nonspecific binding to these sites.

Therefore, we have interpreted the X-ray binding results to be consistent with the solution binding results; i.e., BBAA binds nonspecifically.

(*d*) *Bezafibrate.* Solution binding studies of BZF to dxHb (Figure 4A) indicate a primary class of sites with 2 molecules bound/hemoglobin tetramer. The Scatchard plot (Figure 4A)

also indicates that approximately five additional molecules of BZF bind to a secondary class of binding sites with relatively lower binding constant (see Table IV for comparison).

The X-ray map also indicates one primary class of binding site in the central water cavity with 2 molecules of BZF bound/hemoglobin tetramer. Each BZF molecule was found to span the CFA1 and CFA3 sites. Figure 9A shows the top half of the BZF molecule bound at the CFA1 site (Figure 6A, upper left and lower right density in the central water cavity). Figure 9B shows the bottom half of the BZF molecule bound at the CFA3 site (Figure 6B). Other density exists around the Trp-14α residues in Figure 9A (upper right and lower left) and Trp-15β, but BZF could not be fitted to these sites. We believe that these may be the secondary binding sites observed in the solution studies and perhaps are responsible for the antigelling activity observed for BZF at high concentrations (Abraham et al., 1984).

We conclude that BZF binding and DCBAA binding to dxHb are prototypical of examples illustrating the consistency between solution- and crystal-state binding.

Low versus High Salt Concentration Studies. Our study aimed to also compare the effect of high-salt conditions on the Scatchard plot profiles, the number of binding sites, and the affinity constant of each agent. We only conducted high-salt studies with DCBAA and BZF since they exhibited relatively stronger binding to hemoglobin and their Scatchard plots under low-salt conditions (Figures 1A and 4A) were informative.

This study revealed that the profile of the Scatchard plots is not affected by salt concentration; i.e., the same numbers of binding classes were observed for high- and low-salt DCBAA with HbCO, high- and low-salt DCBAA with dxHb, and high- and low-salt BZF with dxHb (see Figures 1A,B and 4A,B for comparisons). Also, the number of binding sites for each binding class was not affected by the high-salt conditions. However, the binding constant in all cases was notably higher. Table IV demonstrates that K of DCBAA to HbCO was increased from 0.11×10^3 to 0.73×10^3 M^{-1} (7-fold increase) and of DCBAA to dxHb from 0.67×10^3 to 2.85×10^3 M^{-1} (4-fold increase). The BZF binding constants to dxHb for both binding classes were significantly increased by approximately 31-fold (18.75/0.61) for the primary class and by 10-fold (1.36/0.13) for the secondary class.

One possible explanation for the observed increase in the binding constant under high-salt conditions is that high salt concentration helps drive the organic molecules to the friendlier, more hydrophobic environment of the protein.

Locale of Binding–Function Relationship. Earlier studies of these agents (Abraham et al., 1984) revealed that they have an opposite order of antigelling vs allosteric activity (see introduction for details). This reciprocal order of activity prompted us to see if a correlation exists between the locale of binding and the observed activity.

The X-ray results indicate that the allosteric equilibrium will be right shifted (toward a lower affinity for oxygen) when compounds bind to the central water cavity of Hb (examples, BZF and CFA). CFA does have moderate antigelling action, which may be due to the CFA2 site as well as to other nonspecific sites located near the surface. The studied compounds that bind primarily near the surface of the tetramer, away from the central water cavity, appear to have little effect on the allosteric mechanism but do have significant antigelling activity. DCBAA is one good example of this type.

The exhibited multiplicity of binding locales for these compounds was surprising. Although these agents have very close structural similarities, one can see a drastic change in the locale of binding with minimal variation in the structure of the molecule. BBAA and DCBAA best demonstrate this fact. In contrast, the concept of receptor mapping using the classical structure–activity relationship approach depends upon the binding of chemically related molecules to the same site.

Conclusions

We have drawn the following conclusions from this and our previous studies (Abraham et al., 1982, 1983, 1984):

(1) These agents bind differently to the T and R states of hemoglobin. There is more specific binding to T-state hemoglobin.

(2) In general, for this series of molecules, the results of X-ray crystallographic analyses and solution binding studies appear to be consistent.

(3) High-salt conditions used for cocrystallization of hemoglobin with the compounds does not affect either the nature of binding (specific or nonspecific) or the number of sites per class of binding; however, high salt concentrations substantially increase the binding constants.

(4) Small changes in chemical structure of weak binding agents can significantly affect the location of binding on proteins. This may be a general reason for the failure of quantitative structure–activity relationships (QSAR) in other systems.

Acknowledgments

We express our gratitude to Dr. Bonaventura F. Luisi for collecting the X-ray data for DCBAA and to Dr. Max F. Perutz for helpful discussion and advice. We especially thank and acknowledge Dr. Glen Kellogg for his efforts and assistance in drawing the figures.

References

Abraham, D. J., Mehanna, A. S., & Williams, F. L. (1982) *J. Med. Chem. 25*, 1015–1017.

Abraham, D. J., Perutz, M. F., & Phillips, S. E. V. (1983) *Proc. Natl. Acad. Sci. U.S.A. 80*, 324–328.

Abraham, D. J., Kennedy, P. E., Mehanna, A. S., Patwa, D. C., & Williams, F. L. (1984) *J. Med. Chem. 27*, 967–978.

Arnone, A. (1972) *Nature 237*, 146–149.

Blondeau, J. P., & Robel, P. (1975) *Eur. J. Biochem. 55*, 375–384.

Dalziel, K., & O'Brien, J. R. P. (1957a) *Biochem. J. 67*, 119–124.

Dalziel, K., & O'Brien, J. R. P. (1957b) *Biochem. J. 67*, 124–136.

Hofrichter, J., Ross, P. D., & Eaton, W. A. (1976) *Proc. Natl. Acad. Sci. U.S.A. 73*, 3035–3039.

Kent, R. S., DeLean, A., & Lefkowitz, R. J. (1980) *Mol. Pharmacol. 17*, 14–23.

Light, K. E. (1984) *Science 223*, 76–77.

Molinoff, P. B., Wolfe, B. B., & Weiland, G. A. (1981) *Life Sci. 29*, 427–443.

Munson, P. J., & Rodbard, D. (1980) *Anal. Biochem. 107*, 220–239.

Pennock, B. E. (1973) *Anal. Biochem. 56*, 306–309.

Perutz, M. F. (1968) *Cryst. Growth 2*, 54–56.

Perutz, M. F., Fermi, G., Abraham, D. J., Poyart, C., & Bursaux, E. (1986) *J. Am. Chem. Soc. 108*, 1064–1078.

Rosenthal, H. E. (1967) *Anal. Biochem. 20*, 525–532.

Scatchard, G. (1949) *Ann. N.Y. Acad. Sci. 51*, 660–672.

Scheinberg, H. I. (1982) *Science 215*, 312–313.

Scheinberg, H. I., & Armstrong, S. H., Jr. (1950) *J. Am. Chem. Soc. 72*, 535–540, 540–547.